ICAS Paper No. 70-13

A NUMERICAL METHOD FOR TRANSONIC FLOW FIELDS

by
Sune B. Berndt, Professor of Gasdynamics
Royal Institute of Technology
and
Yngve C.-J. Sedin, Aerodynamicist
SAAB Aktiebolag
Sweden

The Seventh Congress of the International Council of the Aeronautical Sciences

CONSIGLIO NAZIONALE DELLE RICERCHE, ROMA, ITALY / SEPTEMBER 14-18, 1970

Price: 400 Lire

A NUMERICAL METHOD FOR TRANSONIC FLOW FIELDS

S.B. Berndt
Royal Institute of Technology
Stockholm, Sweden

and

Y. Sedin
SAAB-SCANIA AB
Linköping, Sweden

Abstract

An iterative method based on the slender-body approximation is applied to the problem of axisymmetric sonic flow. An essential feature is the splitting of the differential equation for the perturbation velocity potential, in regions of subsonic flow, into two coupled parabolic equations which can be integrated stably in alternating radial directions. An outer boundary condition is provided by the asymptotic far-field representation introduced by Guderley and Yoshihara many years ago. - The computations include a number of cases for which experimental data are available. Comparisons with approximate results obtained by other methods are also included. The agreement with experiments is found to be excellent.

1. The Problem

We shall be concerned with the inviscid flow around bodies flying at near sonic speed, in that Mach number range around $M_\infty = 1$ where almost all aircraft are slender from an aerodynamic point of view. It is well known that in order to establish a systematic small-perturbation theory in terms of the thickness ratio τ of such bodies it is highly efficient to use the method of matched asymptotic expansions. Thus, following the body surface inwards when $\tau \to 0$, there arises in this inner limit the slender-body approximation, requiring the computation of a series of two-dimensional harmonic functions in planes perpendicular to the free stream. This is not a difficult task, except for an unknown function of the streamwise coordinate x which can only be determined by matching to an outer approximation. On the other hand, moving outwards (at constant x) in inverse proportion to τ, there arises in that outer limit the classical nonlinear transonic differential equation. It turns out that the matching condition to the inner solution at the body (receding into a segment of the x-axis) contains only the cross-sectional area distribution of the body, in consequence of which the outer approximation, required for completing the slender-body solution, becomes axisymmetric and immediately leads to the transonic equivalence principle as well as the area rule. This is why it is of crucial importance to aeronautical applications of transonic flow theory around $M_\infty = 1$ to be able to solve the axisymmetric problem.

We shall be considering this problem in a normalized form. Let the cross-sectional area distribution of a body under consideration be given by the twice continuously differentiable function $S(x)$, with the origin of x located at the foremost section (behind the leading tip) where $S'' = 0$. Taking $S(0)/S'(0)$ as the unit of length and the free stream velocity as the unit of velocity, and writing the velocity potential in the form $x + \tau^2\varphi$, where $\tau = S'(0)/\sqrt{2\pi S(0)}$, we obtain for the normalized (outer) perturbation potential $\varphi(x, \eta\,;\, k)$ the following problem:

$$\left.\begin{aligned} &\frac{1}{\eta}\frac{\partial}{\partial\eta}(\eta\varphi_\eta) = (k+\varphi_x)\varphi_{xx}\,, \\ &\lim_{\eta\to 0}\eta\varphi_\eta = s'(x), \\ &x^2+\eta^2 \to \infty\,;\ \varphi_x^2+\varphi_\eta^2 \to 0. \end{aligned}\right\} \qquad (1)$$

Here

$$s(x) = S(x)/S(o), \qquad (2)$$

and

$$k = (M_\infty^2 - 1)/\left[M_\infty^2\,\tau^2\,(\gamma+1)\right], \qquad (3)$$

while η, the outer coordinate replacing the radial distance r from the x-axis, is defined by

$$\eta = \sqrt{\gamma+1}\ M_\infty \tau\, r\,, \qquad (4)$$

γ being the specific heat ratio of the fluid (if a perfect gas). This normalization implies that

$$s(0) = s'(0) = 1,\ s''(0) = 0. \qquad (5)$$

The parameter k cannot be suppressed by further normalization; it is an essential parameter of the problem. Large negative values correspond to purely subsonic flow and large positive values to purely supersonic flow. We cannot, nevertheless, define a transonic range in terms of fixed values of k, owing to the singular nature of φ: it will always be possible to find arbitrarily large negative or positive values of φ_x for any value of k by going close enough to the x-axis. The shape of the body therefore is essential in determining how much of transonic flow there is outside the body. This is of no consequence here, however, since we shall be concerned with cases of k approaching zero ("sonic flow"), in which the flow is of a transonic nature out to large distanoe from the body.

One of us recently presented a survey[1] of

this problem of axisymmetric sonic flow around a slender body and of the methods available for solving it, so it is not deemed necessary to do so here. Rather, we shall go directly to our main task of investigating a specific numerical method proposed in that survey, a method based on the slender-body approximation and aimed at providing accurate test solutions to be used when developing simpler methods of approximation.

2. The Approach

The key importance of the slender-body approximation in the present context derives from the fact that this approximation is obtained not only in the inner limit but in all intermediate limits (where, in addition, it is axisymmetric): not until the outer limit does the nonlinear transonic term appear in the limiting differential equation. This suggests, of course, that there is a neighbourhood of the x-axis where φ has the form $\varphi \simeq s'(x)\ln\eta + g(x;k)$, and that this region may extend to a considerable distance. Indeed, analysis of available evidence shows [1] that even as far out as $\eta = 1$ the slender-body approximation is not unreasonable (except for sections where $s(x)$ is not smooth enough, e.g. at the tip of the body, where s'' usually has a jump discontinuity).

The first step of the present method of computation therefore is to substitute for φ two functions, $F(x,\eta;k)$ and $G(x,\eta;k)$, generalizing the η-independent functions s' and g of the slender-body approximation. This is achieved by writing, for $\eta < 1$,

$$F \equiv \eta\varphi_\eta, \quad G \equiv \varphi - \eta\varphi_\eta \ln\eta, \tag{6}$$

which implies that $\varphi = F\ln\eta + G$. From (1), then, follow a system of equations for F and G:

$$\left.\begin{aligned} F_\eta &= \eta\ln\eta\,(k+\ln\eta\,F_x + G_x)(F_{xx} + G_{xx}/\ln\eta), \\ G_\eta &= -\eta\ln\eta\,(k+\ln\eta\,F_x + G_x)(G_{xx} + \ln\eta\,F_{xx}), \\ \eta &= 0\colon\ F = s'(x), \\ \eta &= 1\colon\ G = \varphi(x,1;k) = G\big[F(x,1;k)\big], \end{aligned}\right\} \tag{7}$$

where $G[F]$ denotes the functional relationship between G and F (i.e. φ and φ_x) at $\eta = 1$ as determined by the solution φ for $\eta > 1$. For conciseness, the formulae are not given for the somewhat more general decomposion $\varphi = F\ln(\eta/\eta_m) + G$, $\eta < \eta_m$, although this was in fact used in some of the computations.

It is in line with our surmise of small F_η and G_η to adopt the crude approximation of considering the two differential equations of (7) as parabolic equations for F and G respectively, to be integrated with respect to η. The different signs of the two equations, however, give them different directions of stable integration, so they cannot be integrated together but rather in alternating directions by iteration, keeping G fixed when integrating F_η and vice versa. It is encouraging, then, to note that the apparent coupling between the equations is strong only in regions where the boundary conditions, rather than the differential equations, tend to determine the relationship between F and G. Furthermore, it is the elliptic case ($\varphi_x < 0$) in which the stable directions, outwards for F, inwards for G, are such as to render the boundary conditions into initial conditions. In the hyperbolic case ($\varphi_x > 0$) they would become end conditions, and the scheme would not work; but there we can solve for φ directly by the method of characteristics.

Apart from obvious objections to this somewhat naive approach to a numerical method, there are a number of practical difficulties to overcome, such as obtaining the functional $G[\,]$, locating the sonic line ($\varphi_x = 0$) and fitting in shock waves. In this paper only the simplest case will be considered, namely $k = 0$.

3. The Method for Sonic Flow

The sonic case is simple because there is a limiting characteristic extending to infinity, in front of which there are no shock waves, and because we can obtain $G[\,]$ from the asymptotic far-field representation introduced by Guderley and Yoshihara [2,3]. The situation may be assumed to be as depicted in Fig. 1. The sonic line ($\varphi_x = 0$) starts at the origin (where $s'' = 0$)+ and extends to infinity, crossing the line $\eta = 1$ at C; the limiting characteristic, located farther downstream, starts at the point E on the axis and extends to infinity, crossing $\eta = 1$ at D (neither curve is known in advance, of course). The region downstream of the limiting characteristic is not involved in the problem. The

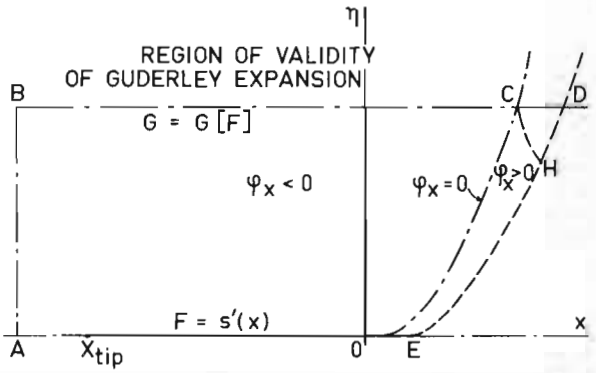

Fig. 1. Regions of integration in the case of sonic flow ($k = 0$).

+ It is one of the important consequences of the presumed validity of the slender-body approximation at the axis that lines of constant φ_x, e.g. the sonic line, $\varphi_x = -k$, can reach the axis only where $s'' = 0$ (hence our choice of origin for x).

relevant part of the hyperbolic region is located between the limiting characteristic and the sonic line, while the problem for φ is elliptic everywhere upstream of the sonic line. The region for alternating integration ($\eta < 1$) is taken to be bounded on the upstream side by a line AB located sufficiently far upstream of the tip of the body (at $x=x_{tip} < -1$) for F to be practically zero at B. It then makes sense to assume the functional G[ ] to be defined approximately over the line segment BD.

The asymptotic far-field representation[2,3], conveniently called the Guderley expansion, may be written

$$\left.\begin{aligned} \varphi(x,\eta;0) &= C^3\left[\eta^{-2/7} f(\zeta) + \sum_{n=2}^{\infty} \alpha_n \eta^{-k/7} f_n(\zeta)\right] \\ \zeta &= C^{-1}(x-x_o)\eta^{-4/7} \\ k &= \sqrt{24n(n+1)+1} - 2n + 1 \end{aligned}\right\} \qquad (8)$$

It consists of a basic solution (the term containing f), which is an exact solution of the transonic differential equation (1) (for k=0), and of a sum of terms obtained by linear perturbation analysis of the basic solution; f and f_n are well-determined functions of ζ, here normalized to place the sonic line of f at $\zeta = 1$. The basic solution is singular at the point $x = x_o$ on the axis; its "strength" is determined by the parameter C. Approximate values, C = .79 and $x_o = -.43$ in the present normalization, were obtained in Ref. 1. However, these parameters, like the coefficients α_n, depend upon the shape of the body and must be determined as part of the solution. The implied validity of the Guderley expansion as far in as $\eta = 1$, suggested by the analysis in Ref. 1, should also be verified by the computions. For further details the reader is referred to the survey in Ref. 1 as well as to Ref. 4, one of several which in recent years have presented analytic expressions for the functions f and f_n.

Now the method of solution can be described by the following prescriptions:

① Obtain, by educated guessing, approximations for the parameters of the Guderley expansion (with a small number of terms), the starting point E of the limiting characteristic, the location of the sonic line for $\eta < 1$, and the function G in the region ABCO.

② Compute by the method of characteristics the solution in the hyperbolic region (OECD), starting with the initial condition for $\eta\varphi_\eta$ (=F) at the axis and keeping the assumed sonic line fixed.

③ Integrate the parabolic equation for F in the elliptic region (ABCO) with G as assumed, starting with the initial values at the axis, obtaining a boundary condition on AB from the Guderley expansion and a boundary condition on the assumed sonic line (OC) from the result of ②.

④ By ② and ③ we have obtained values for $\eta\varphi_\eta$ (=F) on BD: use these for determining C, x_o and a suitable number of coefficients of an improved Guderley expansion, and obtain therefrom values for φ (=G) on BD (thus constructing G[ ]).

⑤ Integrate the differential equation

$$\frac{dx^*}{d\eta} = \frac{-F_x}{\eta\,\varphi_{xx}} , \qquad (9)$$

to obtain a new sonic line $x = x^*(\eta)$. Proceed inwards, starting at the new location C on BD obtained in ④, and using values for F_x and φ_{xx} obtained in ③.

⑥ Integrate the parabolic equation for G in the elliptic region with F as obtained in ③, starting with initial values on BC obtained in ④, obtaining a boundary condition on BA from the improved Guderley expansion and a boundary condition to the left, on the new sonic line, from ⑤.

⑦ Return to ② and proceed, using newly obtained values in place of those guessed in ①.

⑧ Repeat this until the sonic line, as well as F on BD and G on AO, reach stationary values with acceptable precision (or it becomes obvious that the procedure does not converge at all, or not fast enough to be useful).

It ought to be mentioned here that the authors received decisive encouragement to go ahead with this scheme from studying the experiences gained by Yoshihara[5] many years ago in treating numerically the case of a cone-cylinder body.

4. The Numerical Analysis

The following description of the numerical analysis is rather brief and sketchy. Usually, the simplest procedure likely to succeed was chosen for any particular task, and if it did work no attempt was made to improve it. A detailed description of the computer program and its performance was therefore not attempted at this stage.

The flow chart of Fig. 2 names the main procedures of the program - written in ALGOL 60 - and shows how they interact to execute steps ① to ⑧ as outlined above. A great number of special procedures are not shown, such as those evaluating the different fields derived from the Guderley expansion, or those evaluating geometrical data for the body specified in the input. The body contours admitted by the program are those generalized parabolas (degree = n) considered in Ref 7; they include practically all bodies of revolution for which experimental data are available.

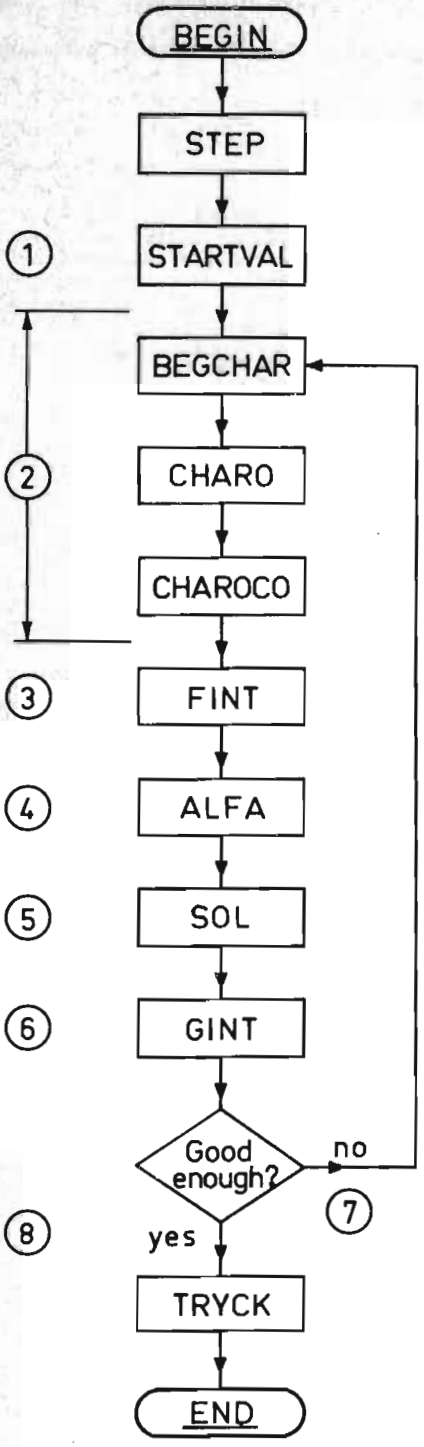

Fig. 2. Flow chart of ALGOL oomputer program.

In the procedure STEP the basic lattice is laid out for the numerical integrations in the elliptic region. Here, as well as in the rest of the program, $\ln\eta$ rather than η is used as the basic radial coordinate. The lattice is a rectangular one with constant step size for both $\ln\eta$ and x. The relationship between the two step sizes is selected by the procedure according to a crude stability criterion based on the stability theory for linear parabolic equations. The first row of lattice points, at $\ln\eta_1$, is put rather close to the axis, typically at $\eta_1 = 0.02$, so that the boundary condition $F = s'(x)$ can be applied there.

The procedure STARTVAL provides the lattice points with starting values as prescribed in ①, using simple slender-body approximations in combination with a Guderley expansion specified in the input.

The program section performing ② is entered by BEGCHAR. It computes the characteristics C_1H_1, leading from the level η_1 down to the level η_0, and starting data along it (see Fig. 3). This is done by assuming the slender-body approximation $\eta\varphi_\eta = s'(x)$.

Having established this starting characteristic and the values of φ_x and $\eta\varphi_\eta$ along it,

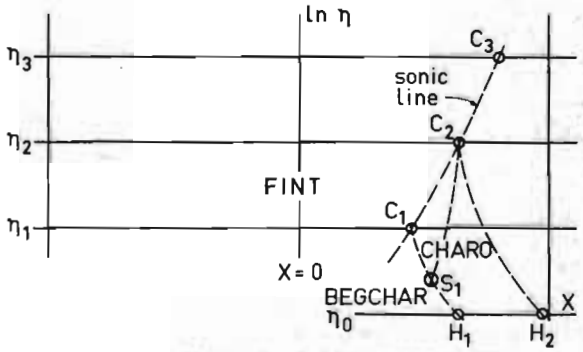

Fig. 3. Characteristics procedures BEGCHAR and CHARO.

the computation proceeds by the characteristics procedure CHARO, which takes us to the next level of η at the sonic line. The procedure makes a three-term series expansion with respect to $\varphi_x^{2/3}$ (a variable naturally suggested by the characteristics equations) in the neighbourhood of the sonic line, and uses this for tracing the characteristic S_1C_2 leading to the assumed sonic point C_2 (at $\eta = \eta_2$), and for computing the values of F, F_x and φ_{xx} at C_2. It thereafter covers the region $H_1C_1C_2H_2$ (or the part of it located upstream of the limiting characteristic; see Fig. 1) to provide data on the characteristic C_2H_2 as a preparation for going to the next η-level. This is repeated until $\eta = 1$ is reached. Finally, the characteristics solution required in

CDH is provided by CHAROCO. It takes boundary values for φ_x on CD (see Fig. 1) from the Guderley expansion and ends up by delivering values for $\eta\varphi_\eta$ on CD.

Next, the parabolic equation for F is integrated by the procedure FINT, using the values obtained from CHARO as a boundary condition for F on the sonic line. FINT is a straightforward three-point centered difference scheme which can be used for either explicit or implicit integration; it contains no special provision for handling the singularity at the tip of the body.

The values for F provided by FINT and CHAROCO on BD are fed into the procedure ALFA, which performs a least squares fitting of the Guderley expansion, thus obtaining new values for C, x_o and a specified number of coefficients α_n. As an auxiliary condition is employed the requirement that the conservation equation

$$\int_{-\infty}^{x^*} \varphi_\eta(x,1)\,dx = 1 + \int_{\text{on sonic line}}^{x^*} F\,dx \,, \qquad (10)$$

easily obtained from (1) and (5), shall be satisfied when the first integral is evaluated by the Guderley expansion and the second by the sonic line data obtained in ②. This serves to give some weight to the values of F upstream of B on $\eta = 1$.

The recomputation of the sonic line is performed by SOL. It integrates (9) by a simple predictor-corrector method, approximating F_x by a linear variation with respect to η in the neighbourhood of the old sonic line (F_x is negative and approaches zero a short distances upstream of the sonic line), while for the longitudinal acceleration, φ_{xx}, is taken the value obtained in CHARO on the downstream side of the old sonic line.

Finally, the integration for G prescribed in ⑥ is performed by GINT. This procedure is essentially identical to FINT, the main difference being that the boundary condition at the sonic line prescribes G_x ($= -F_x \cdot \ln\eta$) rather than G.

This completes the computation program. If the solution needs improving a new round starts at BEGCHAR as prescribed by ⑦, while otherwise the result is printed out in a form determined by TRYCK. It may include, among other things, the values of φ_x and the pressure coefficient C_p at points along the contour of a specified body of revolution and along predetermined lines η =constant, as well as data along the sonic line and the limiting characteristic.

The consistency and precision of the program as described has been tested, in part and in toto, on two different computers, the SAAB D22 and the IBM 360/75. The crucial part of the program, the iterative alternating direction integration in the elliptic region, was found (with a fixed sonic line) to be stable and to converge rapidly towards a staticnary solution. The sonic line, on the other hand, does not seem to be quite as welldetermined, most likely due to the influence of truncation errors in satisfying the condition of continuous φ_x across the sonic line. However, the effect on the pressure distribution at the body seems to be entirely negligible within the precision aimed at in the present preliminary computations, namely one step better precision than that of available experimental data. 'Simple precision', as available in the two computers, was found to be amply adequate, throughout.

Based on these tests the following choice was made for the parameters of the program:

STEP: $\Delta x = 0.2$, $\eta_1 = 0.02$;

BEGCHAR: $\eta_o = 0.001$

FINT and GINT: explicite integration

ALFA: $n \leq 5$

Exit Condition: change of $|G_x(0,1)|$ from preceeding step $< .01$.

In most cases this setup led to four iterations and a computer time (CPU) of 6 minutes; the core memory space required was 250K (on the IBM 360/75).

The tests leave little doubt that a more efficient program will permit considerable saving of computer time and memory space with the same or improved precision.

5. Results

The fact that the output from our computational scheme seems to converge rapidly towards a welldetermined end result does not, of course, guarantee that the result is close to a solution of the original problem (if such a solution does indeed exist). Rather, in view of the nonlinear character of the problem and the complexity of the method, there would seem to be a considerable risk of arriving at a spurious result. Since there is no exact solution available for comparison, the only way to find out seems to be to compare with experimental results. But that might not be a bad way: if the method passes such a test we may, in fact, contend that we have proved not only the numerical method but also the original perturbation analysis.

The experimental results available at $M_\infty = 1$ are mainly for bodies of revolution at zero incidence. Our computation of the outer solution φ should be immediately applicable to such bodies since it happens to contain the inner solution (as far as the differential equation and the boundary condition are concerned). It is only in computing the state of the gas in

the neighbourhood of the body that additional terms appear, namely terms proportional to the square of the crossflow velocity. For example, the following formula is valid for the pressure coefficient,

$$C_p = -2\tau^2\left[\varphi_x + \left(\frac{r_o s'}{2r}\right)^2\right] \qquad (11)$$

(r_o=body radius at x=0), while similar additions must made when locating the sonic line and the characteristics at the body (see e.g. Ref. 1).

Material for comparison was selected from the experimental data of McDevitt and Taylor[6,7]. These are the most complete ones available (they cover, in fact, much of the data available from other sources, e.g. Ref. 8). The bodies tested, having different location ξ of the maximum thickness, are described in Table 1. As mentioned earlier, n is the degree of the generalized parabola defining the body contour. For the precise definition of ξ and f ("fineness ratio" $\propto 1/\tau$) the reader is referred to Ref. 7.

TABLE 1. Geometrical data of bodies of revolution

ξ	n	f	τ	x_{tip}	$s''(x_{tip})$	$s'''(0)$
0.3	6.03	12	0.271	-1.42	1.75	-0.61
0.4	3.39	12	0.184	-1.44	1.60	-0.67
0.5	2	10	0.163	-1.46	1.50	-0.75
		12	0.136			
		14	0.117			
0.6	3.39	12	0.104	-1.61	0.90	-1.18
0.7	6.03	12	0.086	-1.75	0.69	-1.93

However, there is strong indication[10] that the data for the three last bodies are considerably influenced by wall interference. That leaves essentially the three first bodies for an accurate comparison. But those are so similar in shape that it would not seem worth while to consider all of them. Therefore, only the first and third bodies were selected.

In fact, it was thought sufficient to restrict the presentation here to the third body, leaving the first one for the oral presentation. This is done in Fig. 4, which shows the pressure distribution on the forward part of the body and along the lines η = 0.175 and 0.351. The agreement at the body surface is rather good. Away from there deviations are seen: primarily, the influence of the body does not propagate as strongly upstream in the experiments as in the computations. This effect might well be due to the presence of the slotted walls of the wind tunnel, but wether this is the true explanation

+ The variation of τ is not significant, of course: the data are known to be consistent with the transonic similarity rule[18].

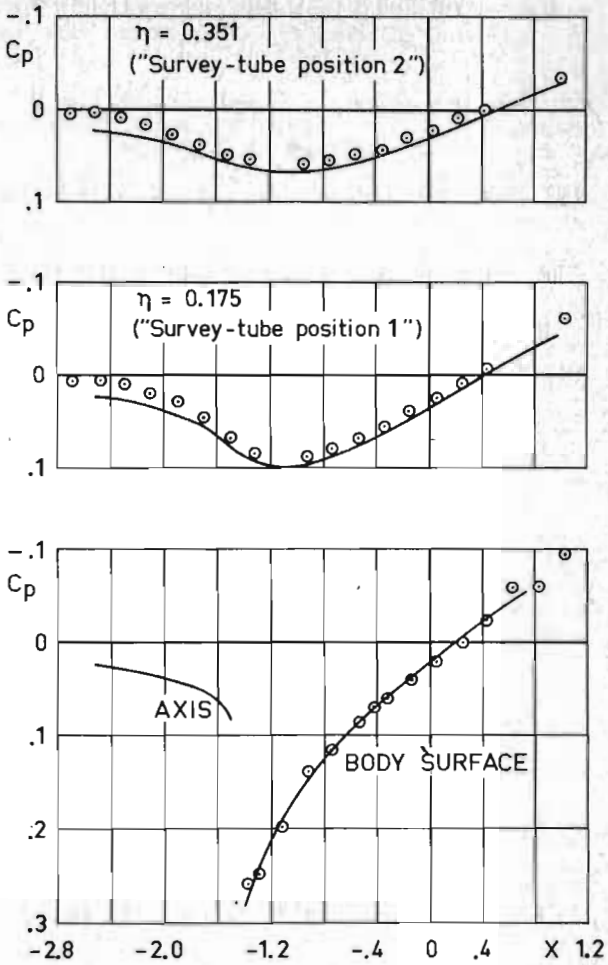

Fig. 5. Computed pressure distribution on parabolic-arc body (n=2) of fineness ratio f = 10, and along lines η = 0.175 and 0.351 (experimental points from Ref. 6).

or the computations are inaccurate, cannot be decided at this stage.

A comparison with results obtained by other methods of computation could be interesting. All such methods seem to derive from the so-called parabolic method of Oswatitsch and Keune[11], the most accurate of them being the local-linearization method of Spreiter and Alksne[9]. This method is known to give results which agree very well with experiments, so for the bodies selected above the results are bound agree with those of the present method as well. The situation might be different for the last two bodies of Table 1, however, since no accurate experimental data are available for those. Results from the local-linearization method are available

for the last body[10] they are compared with results from the present method in Fig. 6. There is seen to be a small systematic deviation. What it means cannot be ascertained at this stage. The answer might be obtained from improving the accuracy of the present method, or from making an assessment of the wall interference so that experimental data may be called in again.

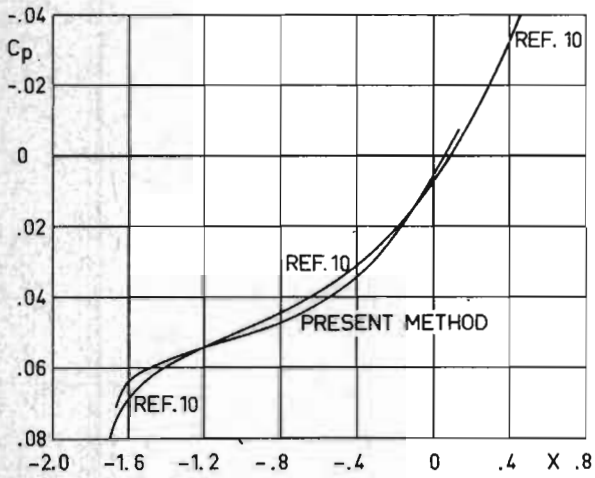

Fig 6. Computed pressure distributions on body of fineness ratio f = 12 having maximum thickness at $\xi = 0.3$.

6. Conclusions

The results obtained so far are rather encouraging and seem to indicate that the method developed will make possible accurate computation of axisymmetric flows at $M_\infty = 1$ with a reasonable computing effort. What remains to be done is essentially to revise the computer program for higher efficiency, and to calibrate its precision and performance in terms of program parameters.

There is an obvious need for extending the method so as to be able to treat the effect of wind tunnel walls. Another useful development to attempt would be to find methods for describing the far field accurately at $M_\infty \neq 1$, as would be needed för extending the method to subsonic and supersonic transonic flows. More generally, the success of the method of alternating direction integration indicates that it might be a useful tool even outside the transonic small-perturbation theory.

Acknowledgments

The authors want to express their thanks to a number of collaborators, in particular to Roine Mattsson and Jörgen Andersen who made a decisive contribution in debugging and developing the computer program.

References

1. Berndt, S.B., An approach to the problem of axisymmetric sonic flow around a slender body. Proc. 12th Int. Congr. Appl. Mech., Stanford Un. 1968; Berlin/Heidelberg/New York: Springer 1969, p. 135

2. Guderley, K.G. and Yoshihara, H., An axial-symmetric transonic flow pattern. Qu.Appl. Math. 8, 333 (1951)

3. Guderley, K.G., Axial symmetric flow patterns at a free stream Mach number close to one. US Air Force Tech. Rep. No. 6285 (1950)

4. Randall, D.G., Some results in the theory of almost axisymmetric flow at transonic speed. AIAA J. 3, 2339 (1965)

5. Yoshihara, H., On the flow over a cone-cylinder body at Mach number one. WADC Tech. Rep. 52-295 (1952)

6. Taylor, R.A. and McDevitt, J.B., Pressure distributions at transonic speeds for parabolic-arc bodies of revolution having fineness ratios of 10, 12 and 14. NACA TN 4234 (1958)

7. McDevitt, J.B. and Taylor, R.A., Pressure distributions at transonic speeds for slender bodies having various axial locations of maximum diameter. NACA TN 4280 (1958)

8. Drougge, G., An experimental investigation of the interference between bodies of revolution at transonic speeds with special reference to the sonic and supersonic area rules. Aero. Res. Inst. of Sweden (FFA), Rep 83 (1959)

9. Spreiter, J.R. and Alksne, A.Y., Slender-body theory based on approximate solution of the transonic flow equation. NASA Rep. 2 (1959)

10. Spreiter, J.R., Smith, D.W., and Hyett, B.J., A study of the simulation of flow with free-stream Mach number 1 in a choked wind tunnel. NASA TR R-73 (1960)

11. Oswatitsch, K., and Keune, F., The flow around bodies of revolution at Mach number one. Proc. of Conf. on High-Speed Aeronautics, Polytechnic Inst. of Brooklyn, 1955, p. 113.